A new approach to fuzzy location of cephalometric landmarks in craniofacial superimposition

Oscar Ibáñez[1] Oscar Cordón[1] Sergio Damas[1] Sergio Guadarrama[1] José Santamaría[2]

[1]European Centre for Soft Computing. Mieres, Spain
[2]Computer Science Department, University of Jaén. Jaén, Spain
Email: {oscar.ibanez,oscar.cordon,sergio.damas,sergio.guadarrama}@softcomputing.es, jslopez@ujaen.es

Abstract— *Craniofacial superimposition is the second stage of a complex forensic technique that aims to identify a missing person from a photograph (or video shot) and the skull found. This specific task is devoted to find the most appropriate pose of the skull model to be projected onto the photograph. The process is guided by a number of landmarks identified both in the skull (craniometric landmarks) and in the face (cephalometric landmarks). In this contribution we extend our previous genetic algorithm-based approach to the problem by considering the uncertainty involved in the location of the cephalometric landmarks and its influence in the matching between these landmarks and the craniometric ones. The new proposal is tested over two instances of a real case solved by the Physical Anthropology lab at the University of Granada (Spain).*

Keywords— Craniofacial superimposition, fuzzy landmarks, genetic algorithms, image registration.

1 Introduction

Photographic supra-projection [1] is a forensic process where photographs or video shots of a missing person are compared with the skull that is found. By projecting both photographs on top of each other (or, even better, matching a scanned three-dimensional skull model against the face photo/video shot), the forensic anthropologist can try to establish whether that is the same person. To do so, an accurate 3D model of the skull is first demanded. Next, the matching of two sets of radiometric points (facial anthropometric landmarks in the subject photograph, and cranial anthropometric landmarks in the obtained skull model) is considered to guide the superimposition of the skull 3D model and the face photograph [1]. Then, a decision making stage starts by analyzing the different kinds of achieved matches between landmarks. Due to physiognomic characteristics, some of them will perfectly match, some will partially do so, and finally some others will not. After the whole process, the forensic expert must declare whether the analyzed skull corresponds to the missing person or not.

This procedure is very time consuming and there is no systematic methodology but every expert often applies a particular process. Hence, there is a strong interest in designing automatic methods to support the forensic anthropologist to put it into effect. In a previous proposal [2], we tackled the second stage of the process, i.e. the craniofacial superimposition, by means of evolutionary algorithms assuming no uncertainty was involved in the process. Next, in [3] we identified two sources of uncertainty in the problem. On the one hand, the *landmark matching uncertainty* (not yet modeled in any of our works) will refer to the imprecision involved in the matching of the landmarks that correspond to the two different objects: the face and the skull (as said, there is a clear partial matching situation). On the other hand, the *landmark location uncertainty* is related to the extremely difficult task of locating the landmarks [4] in an invariable place, with the accuracy required for this application. Indeed, every forensic anthropologist is prone to locate the landmarks in a slightly different position. The ambiguity may also arise from reasons like variation in shade distribution depending on light condition during photographing, unsuitable camera focusing, poor image quality, etc.

In our previous contribution [3], we tackled the landmark location uncertainty considering the cephalometric landmarks as rectangular zones of different sizes, instead of using crisp locations, taking inspiration from [5]. However, this is a too simple way to represent the underlying uncertainty since all the posible crisp points in the rectangle are equally likely to be the actual location, which is not so realistic.

In this contribution we will improve the previous approach by using fuzzy sets to model the uncertainty related to each cephalometric landmark location. In addition, we will also consider fuzzy distances to model the distance between each pair of craniometric and cephalometric landmarks. The resulting genetic fuzzy system [6] is tested on two superimposition problems derived from a real-world identification case solved by the Physical Anthropology lab at the University of Granada.

The structure of the contribution is as follows. Section 2 is devoted to review our previous proposal on evolutionary craniofacial superimposition. Our new proposal is described in Section 3. Then, Section 4 presents the experimental study. Finally, Section 5 collects some concluding remarks and future works.

2 Real-coded genetic algorithm for craniofacial superimposition

In [2] we first formulated this complex task in forensic identification as a numerical optimization problem related to the well known field of image registration (IR) [7]. Then we adapted three different evolutionary algorithms to solve it: two variants of a real-coded genetic algorithm (GA) and an evolution strategy.

A sensible way to design an automatic craniofacial superimposition procedure is through the use of a IR technique to properly align the 3D skull model and the 2D face photograph in a common coordinate frame. Taking a previous proposal [8] as a base, we modeled the required perspective transformation as a set of geometric operations involving translation, rota-

ISBN: 978-989-95079-6-8

tion, scaling and projection. That registration transformation is defined by 12 parameters which are encoded in a real-coded chromosome. The search for the best transformation parameters is guided by a number of pairings between craniometric and cephalometric landmarks located in the skull and the face, respectively.

Different definitions of the objective function were studied and the one achieving the best results was the mean error[1]:

$$ME = \frac{\sum_{i=1}^{N} ||f(cl^i) - fl^i||}{N} \quad (1)$$

where $||\cdot||$ is the 2D Euclidean distance, N is the number of considered landmarks (only four in Nickerson et al.'s proposal), cl^i corresponds to every 3D craniometric landmark, fl^i refers to every 2D facial landmark, f is the function which defines the geometric 3D-2D transformation, and $f(cl^i)$ represents the position of the transformed skull 3D landmark cl^i in the projection plane.

Among the three different evolutionary designs developed to solve the problem, a real-coded generational GA using tournament selection [9], Simulated Binary crossover (SBX) [10] and random mutation operators [11] was proposed and is the one considered in this contribution.

Later on, we introduced the uncertainty treatment in the location of cephalometric landmarks [3]. In that first approach, based on the work by Sinha [5], we considered the cephalometric landmarks as rectangular zones, instead of using crisp locations. The larger the rectangle that defines each landmark, the lower the contribution of the corresponding landmark to the fitness function. Finally, we calculated the Euclidean distances between craniometric and cephalometric landmarks, using the centroid of the rectangle related to the uncertain ones. Thus, once the centroid of the uncertain landmarks was considered, the problem of computing distances between a set of uncertain landmarks and a set of crisp ones became the problem of measuring a set of Euclidean distances between different pairs of crisp landmarks. That was just a first approach to model the location uncertainty, which did not take into account the inherent uncertainty involved when we are measuring distances between fuzzy and crisp points.

3 New proposal for the fuzzy location of cephalometric landmarks

The use of fuzzy landmarks in this contribution aims to face the landmark location uncertainty in the photograph of the missing person. Furthermore, the present approach also deals with the uncertainty involved when distances between crisp points and fuzzy ones are measured, as a consequence of the fact that craniometric landmarks are considered as crisp values[2]. In order to cope with the fact that each forensic expert could place each facial landmark in different positions in the 2D image, the higher the uncertainty related to a landmark, the broader the region where the forensic experts would locate that landmark in the photograph.

[1]Notice that, mean square error is not used because of its negative effect when image ranges are normalized in [0,1]

[2]As said, we have not considered the location uncertainty in craniometric landmarks due to the big resolution (one mm per pixel) and high quality of the 3D skull model.

In addition, by using fuzzy landmarks, those experts are able to locate a larger set of landmarks with the proper level of confidence (using fuzzy regions of different sizes). In contrast, following the classical crisp approach, they would only be able to mark the landmarks whose position they can determine precisely. Due to different reasons as the pose of the missing person, the quality of the image, or partial occlusions of landmark regions, it can be difficult to do so for many of the existing cephalometric landmarks. Hence, this approach presents an important advantage since the bigger the set of landmarks, the more complete the information will be to guide the genetic search of the best transformation to properly superimpose the skull on the photograph. In this way, it will also allow us to improve the performance of our previous proposal in some problematic instances with several specific poses (see Figures 4 and 8).

To ease the comprehension of our formulation to the reader, we review some required basic concepts from Fuzzy Sets Theory [12] as follows. For each $\alpha \in (0,1]$ the α-level set $\widetilde{A}_\alpha$ of a fuzzy set $\widetilde{A}, \mu_{\widetilde{A}} :\rightarrow [0,1]$, is $\widetilde{A}_\alpha = \{x \in X; \mu_{\widetilde{A}(x)} \geq \alpha\}$. Hence, the core $\widetilde{A}_1 = \{x \in X; \mu_{\widetilde{A}(x)} = 1\}$ of a fuzzy set is the subset of X whose elements have membership equal to 1. The support $\widetilde{A}_0$ is defined as the closure of the union of all its level sets, that is

$$\widetilde{A}_0 = \overline{\bigcup_{\alpha \in (0,1]} \widetilde{A}_\alpha}$$

3.1 Distance between a point and a set of points

Given a point x of $\mathbb{R}^n$ and a nonempty subset A of $\mathbb{R}^n$ we can define a distance $d : \mathbb{R}^n \times \mathbb{P}(\mathbb{R}^n) \rightarrow \mathbb{R}^+$ by:

$$d(x, A) = inf\{||x - a||; a \in A\}$$

for a certain norm $||.||$ on $\mathbb{R}^n$. Thus, $d(x, A) \geq 0$ and $d(x, A) = 0 \Rightarrow x \in A$.

3.2 Distance between a point and a fuzzy set of points

Now we can define the distance between a point x of $\mathbb{R}^n$ an a fuzzy set of points $A : \mathbb{R}^n \rightarrow [0,1]$ by:

$$d^*(x, \widetilde{A}) = \int_0^1 d(x, \widetilde{A}_\alpha) d\alpha$$

Lemma 3.1. *The distance from the point x to the fuzzy set $\widetilde{A}$ is lesser or equal than the distance to the core of $\widetilde{A}$ and greater or equal than the distance to the support of $\widetilde{A}_0$. That is,*

$$d(x, \widetilde{A}_1) \leq d^*(x, \widetilde{A}) \leq d(x, \widetilde{A}_0)$$

The proof is straight forward.

In case that we have discrete fuzzy set of points $\widetilde{A} = x_1/\alpha_1 + \cdots + x_m/\alpha_m$, the distance can be expressed by:

$$d^*(x, \widetilde{A}) = \frac{\sum_{i=1}^{m} d(x, \widetilde{A}_{\alpha_i}) * \alpha_i}{\sum_{i=1}^{m} \alpha_i}$$

Following the idea of metric spaces in [13] we will define a fuzzy landmark as a fuzzy convex set of points having a

ISBN: 978-989-95079-6-8

nonempty core and a bounded support. That is, all its α-levels are nonempty, bounded and convex sets.

In our case, since we are dealing with 2D photographs with an $x \times y$ resolution, we can define the fuzzy landmarks as 2D masks represented as a matrix m with $m_x \times m_y$ points. Each fuzzy landmark will have a different size depending on the imprecision on its localization but at least one pixel (i.e. crisp point related to a matrix cell) will have membership with degree one. An example of a 5×5 mask is:

	1	2	3	4	5
1	0.1	0.3	0.5	0.3	0.1
2	0.3	0.5	0.7	0.5	0.3
3	0.5	0.7	1	0.7	0.5
4	0.3	0.5	0.7	0.5	0.3
5	0.1	0.3	0.5	0.3	0.1

These masks are easily built starting from two triangular fuzzy sets $\widetilde{V}$ and $\widetilde{H}$ representing the approximate vertical and horizontal position of the landmark, thus becoming two-dimensional fuzzy sets. Each triangular fuzzy set $\widetilde{A}$, is defined by its center c and its offsets l, r as follows:

$$\widetilde{A}(x) = \begin{cases} 1 - \frac{|x-c|}{c-l}, & \text{if } l \leq x \leq c \\ 1 - \frac{|x-c|}{r-c}, & \text{if } c < x \leq r \\ 0, & \text{otherwise} \end{cases}$$

and the membership functions of the fuzzy landmarks are calculated using the product t-norm by:

$$\mu_{\widetilde{F}}(i,j) = \mu_{\widetilde{V}}(i) \cdot \mu_{\widetilde{H}}(j)$$

Now we can calculate the distance between a point (which will be the projection of the 3D craniometric landmark on the 2D face photo) and the fuzzy landmark (representing the position of the cephalometric landmark), as depicted in Figure 1. Note that the implemented distance between a point and a fuzzy set of points is quite similar to the one defined in [14].

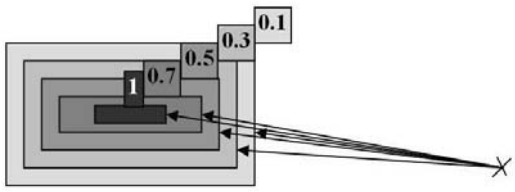

Figure 1: Distance between a point and a fuzzy point

If we denote as $d_i = d(x, \widetilde{F}_{\alpha_i})$ the distance from point x to the α-level set $\widetilde{F}_{\alpha_i})$, then the distance from the point to the fuzzy landmark $\widetilde{F}$, can be expressed by:

$$d^*(x, \widetilde{F}) = \frac{\sum_{i=1}^{m} d_i \cdot \alpha_i}{\sum_{i=1}^{m} \alpha_i}$$

In the example of Figure 1, taking $\{\alpha_1 = 0.1, \alpha_2 = 0.3, \alpha_3 = 0.5, \alpha_4 = 0.7, \alpha_5 = 1\}$ and assuming $\{d_1 = 4.5, d_2 = 5.4, d_3 = 6.3, d_4 = 7.3, d_5 = 9\}$, we calculate the distance as:

$$d^*(x, \widetilde{F}) = \frac{d_1 \cdot \alpha_1 + \cdots + d_5 \cdot \alpha_5}{\alpha_1 + \cdots + \alpha_5} = \frac{19.33}{2.6} = 7.43$$

Therefore, we have modified the previous definition of our genetic craniofacial superimposition techniques's fitness function (see section 2) as follows:

$$\textit{fuzzy ME} = \frac{\sum_{i=1}^{N} d^*(f(cl^i), \widetilde{F}^i)}{N} \quad (2)$$

where N is the number of considered landmarks, cl^i corresponds to every 3D craniometric landmark, f is the function which defines the geometric 3D-2D transformation, $f(cl^i)$ represents the position of the transformed skull 3D landmark cl^i in the projection plane, that is to say, a crisp point. $\widetilde{F}^i$ represents the fuzzy set points of each cephalometric landmark and finally, $d^*(f(C_i), \widetilde{F}^i)$ is the distance between a point and a fuzzy set points.

4 Experiments

After explaining the sources of uncertainty and our proposal to deal with the landmark location uncertainty, we will study its performance as follows. Section 4.1 presents the considered experimental design. Sections 4.2 and 4.3 are devoted to the analysis of one real-world case of study with two different photographs (two different poses).

4.1 Experimental design

Two different types of landmark sets for our case of study were provided by the forensic experts. The first type is the one classically used in the manual superimposition process. It is composed of crisp landmarks, those the forensic anthropologists can place in a single pixel. The second one is a set of fuzzy landmarks, that is to say, a region for each landmark. As said, in this second set, the forensic expert could place more landmarks than in the first one, due to the possibility of drawing bigger (in size) fuzzy sets of points. Notice that, in the former case, the forensic anthropologist would only identify those landmarks which are clearly located in a specific pixel without any doubt. According to different criteria concerning the features of both the considered landmarks and the photograph characteristics (pose, quality, etc.), forensic experts used areas of different size to determine the position of each landmark in that second set.

We compare the results of the genetic craniofacial superimposition based on crisp landmarks with those reached by using fuzzy location of cephalometric landmarks. In order to perform a significant and fair comparison between crisp and fuzzy approaches concerning the number of landmarks, we considered the following experimental design: two different sets of fuzzy landmarks are used, one with the same size (and, of course, the same specific landmarks) as the crisp set and another also including the additional landmarks identified thanks to the use of the fuzzy location approach.

The case study is a real-world one happened in Cádiz, Spain. The skull 3D model (327,641 points stored as x, y, z coordinates), see Figure 2, was acquired using Konica-Minolta 3D Lasserscanner VI-910. Two photographs[3] were provided by the family (see Figures 2 and 6). They were acquired at different moments and in different poses and conditions. Hence this case consists of two distinct superimposition

[3]Notice that we have processed the photographs to hide the subject identity following legal issues.

ISBN: 978-989-95079-6-8

problems. It was initially solved following a manual approach. The forensic experts tried to use both photographs but finally they were restricted to only one of them (pose 1 photograph), because they did not achieve a proper superimposition for the second due to the face pose.

Experiments consider the best performing GA parameter values in [2]: number of generations = 600, population size = 1,000, SBX η parameter = 1, mutation probability = 0.2, crossover probability = 0.9, and tournament size = 2. For all the tests, 30 runs of the GA are considered. Tables 1 and 2 show the minimum (m), maximum (M), mean (μ) and standard deviation (σ) of ME relative to the Euclidean distances between cephalometric landmarks and the transformed craniometric landmarks achieved by the GA. Notice that, in the case of crisp landmarks, the fitness function is directly defined as the "crisp" ME. However, when we use fuzzy landmarks the fitness function is not the ME, but a fuzzy distance between the transformed skull landmarks and the fuzzy regions (the average of the fuzzy distances). Owing to that, numerical results are not fully comparable. Nevertheless, we present the ME values in both cases as the only way to provide an error measurement.

4.2 Case study 1, pose 1

Figure 2 depicts this data set. In this first pose, the anthropologists identified nine crisp cephalometric landmarks. In addition, they marked these nine landmarks following a fuzzy approach, which also allowed them to identified a new set with five more (see Figure 3). Specially recall the large amount of fuzziness of the *vertex* landmark, located in the top part of the head. There is a strong uncertainty on its location due to the woman's hair and the forensic expert would have never trusted in that landmark in case a crisp location have to be defined. The corresponding craniometric landmarks were manually extracted from the skull 3D model.

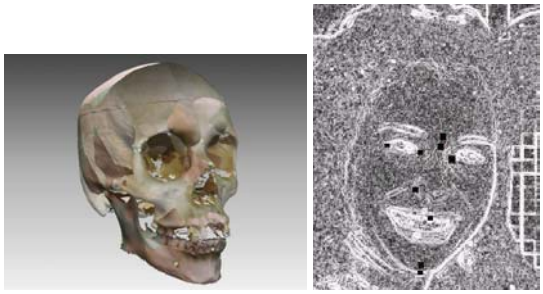

Figure 2: Case study 1, pose 1. 3D model of the skull (left) and photograph of the missing person with a set of nine crisp landmarks, represented by squares (right).

Table 1 presents the ME values for the obtained craniofacial superimpositions, distinguishing between crisp and fuzzy locations. It is important to remind that results are not fully comparable since the superimposition process using fuzzy landmarks does not minimize the ME but a different function (see Equations 1 and 2). Figures 4 and 5 present the best superimposition results of the crisp and the fuzzy approaches to allow a visual comparison.

On the one hand, referring to the numerical results, a very similar behavior is observed. Both approaches demonstrate a robust conduct. Notice that, in the case of the larger set of landmarks (fourteen fuzzy landmarks), Table 1 shows the ME corresponding just to the nine landmarks it shares with the smaller sets of landmarks. This higher ME value demonstrates that a larger error (i.e., distance between landmarks) value not necessarily means a worst superimposition (as we will see below). On the other hand, visual superimposition results show again a very similar behavior in both approaches for a smaller set of landmarks (Figure 4). These results are unacceptable for identification purposes. Finally, we can clearly identify the improvement in the superimposition when a larger set of fuzzy landmarks is used (Figure 5). Our forensic anthropologists confirmed the final superimposition result is good enough to be used in the final decision making stage of the photographic supra-projection process.

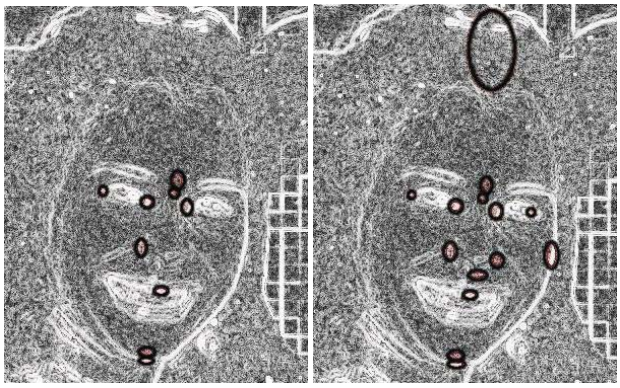

Figure 3: Case study 1, pose 1. Photograph of the missing person with two different sets of fuzzy landmarks: one of nine (left) and the other with fourteen (right) fuzzy landmarks. Landmarks are represented by ellipses.

Table 1: Case study 1, pose 1. Superimposition results.

Landmark set	ME			
	m	M	μ	σ
Nine crisp l.	0.0083	0.0086	0.0084	0.0000
Nine fuzzy l.	0.0084	0.0334	0.0095	0.0045
Fourteen fuzzy l. (ME over nine)	0.0122	0.0133	0.0124	0.0002

Figure 4: Case study 1, pose 1. Best superimposition results achieved using nine crisp (left) and nine fuzzy (right) landmarks, respectively.

ISBN: 978-989-95079-6-8

Figure 5: Case study 1, pose 1. Best superimposition result achieved using fourteen fuzzy landmarks.

4.3 Case study 1, pose 2

In this second pose, the anthropologists originally identified twelve crisp cephalometric landmarks following a crisp approach (see Figure 6). They also marked three more landmarks following a fuzzy approach. Figure 7 depicts both sets of fuzzy landmarks.

Figure 6: Case study 1, pose 2. Photograph of the missing person with the corresponding set of twelve crisp landmarks.

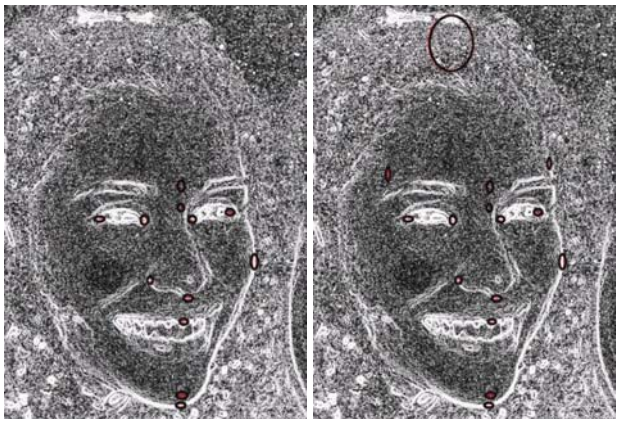

Figure 7: Case study 1, pose 2. Photograph of the missing person with two different sets of fuzzy landmarks, twelve (left) and fifteen (right).

Table 2 presents the ME figures for the obtained craniofacial superimpositions. In spite of the different fitness functions minimized, a very similar behavior is observed. As in the previous pose, the ME value of the larger set of landmarks was calculated just using the twelve landmarks that compose the smaller set. Both approaches demonstrate a robust conduct. Besides, it can be recognized how the fuzzy approach becomes more robust when considering a larger set of landmarks. On the other hand, Figure 8 presents the visual representations of the superimposition results which again show a very similar bad behavior in both approaches for a reduced set of landmarks. Finally, we can clearly see the improvement in the superimposition when a larger set of fuzzy landmarks is used (Figure 9, left). The final superimposition result is good enough to be used in the following decision making stage. In fact, this automatic superimposition is much better than that manually achieved by the forensic anthropologists (Figure 9, right), which was restricted by the computer vision tools they considered and by the lateral pose of the face photograph. The latter issues forced them to discard this photograph in the identification decision.

Table 2: Case study 1, pose 2. Superimposition results obtained using crisp and fuzzy locations

Landmark set	ME			
	m	M	μ	σ
Twelve crisp l.	0.0347	0.0354	0.0350	0.0002
Twelve fuzzy l.	0.0343	0.0613	0.0357	0.0048
Fifteen fuzzy l. (ME over twelve)	0.0382	0.0412	0.0391	0.0001

Figure 8: Case study 1, pose 2. Best superimposition results achieved using twelve crisp (left) and fuzzy (right) landmarks.

5 Concluding remarks and future works

We have proposed the use of fuzzy landmarks to tackle the uncertainty related to landmark location for a complex forensic identification task called craniofacial superimposition. We have used two different sets of landmarks provided by the forensic anthropologists for two photographs of the same identification case. We have compared the automatic superimpositions obtained by a GA considering crisp landmarks and those achieved using fuzzy landmarks. Promising results have been achieved following a fuzzy approach, showing that it is

ISBN: 978-989-95079-6-8

Figure 9: Case study 1, pose 2. Best superimposition result achieved using fifteen fuzzy landmarks (left) and best manual superimposition obtained by the forensic experts (right).

able to model the inherent uncertainty involved in the location of the landmarks. None of the achieved results following a crisp approach provided a better superimposition than the fuzzy approach. Thus, our proposal becomes more robust when tackling different locations of the landmarks.

By using fuzzy landmarks, forensic experts are able to place a larger landmark set with the proper level of confidence (using different sizes for the landmarks representing different levels of uncertainty in their actual location). In contrast, following the classical crisp approach, they are only able to mark those landmarks whose position they are able to determine precisely. As we expected, results show a much better performance of the GA when the number of landmarks is larger and that was only possible by using fuzzy location of landmarks.

As a drawback, the fuzzy approach implies more computational operations with the consequent increment in the run time required for the GA: from the 20-40 seconds per run using crisp landmarks to the 2-4 minutes using fuzzy landmarks. However, it is still a significantly short time if we compare it with the usual time needed by the forensic experts to perform a manual superimposition, around 24 hours.

Besides, these results need to be confirmed in a more extensive study, with a larger number of cases and using other different fuzzy distances [15]. As additional future work, we aim to determine the specific transformation parameters of the manual superimposition achieved by the forensic expert. We will use those parameters as the ground truth solution to measure the accuracy of the automatic superimposition processes. We will also make a poll between different forensic anthropologists in order to define the most appropriate shapes and sizes for the fuzzy landmarks in several face photographs corresponding to real-world previously solved cases. That poll will be also helpful in order to have different sets of crisp landmarks for comparison purposes. In addition, we are planning to introduce the landmark matching uncertainty (see Section 1). Finally, we aim to tackle the identification stage, i.e. the final decision making process, by using fuzzy logic, in order to assist the forensic expert in the final identification decision.

Acknowledgments

This work was partially supported by the Spain's Ministerio de Educación y Ciencia (ref. TIN2006-00829) and by the Andalusian Dpto. de Innovación, Ciencia y Empresa (ref. TIC1619), both including EDRF funding. We want to acknowledge all the team of the Physical Anthropology lab at the University of Granada (headed by Dr. Botella and Dr. Alemán) for their support during the data acquisition and validation processes. Dr. Guadarrama's work has been supported by the Spanish Department of Science and Innovation (MICINN) under program Juan de la Cierva JCI-2008-3531, and the European Social Fund.

References

[1] M. Y. Iscan. Introduction to techniques for photographic comparison. In M. Y. Iscan and R. Helmer, editors, *Forensic Analysis of the Skull*, pages 57–90. Wiley, 1993.

[2] O. Ibáñez, L. Ballerini, O. Cordón, S. Damas, and J. Santamaría. An experimental study on the applicability of evolutionary algorithms to craniofacial superimposition in forensic identification. *Information Sciences,* in press*, http://dx.doi.org/10.1016/j.ins.2008.12.029*, 2009.

[3] O. Ibáñez, O. Cordón, S. Damas, and J. Santamaría. Craniofacial superimposition based on genetic algorithms and fuzzy location of cephalometric landmarks. In *Hybrid artificial intelligence systems*, number 5271 in LNAI, pages 599–607, 2008.

[4] J. Richtsmeier, C. Paik, P. Elfert, T.M. Cole, and F. Dahlman. Precision, repeatability and validation of the localization of cranial landmarks using computed tomography scans. *The Cleft Palate-Craniofacial Journal*, 32(3):217–227, 1995.

[5] P. Sinha. A symmetry perceiving adaptive neural network and facial image recognition. *Forensic Science International*, 98(1-2):67–89, November 1998.

[6] O. Cordón, F. Gomide, F. Herrera, F. Hoffmann, and L. Magdalena. Ten years of genetic fuzzy systems: Current framework and new trends. *Fuzzy Sets and Systems*, 141(1):5–31, 2004.

[7] B. Zitova and J. Flusser. Image registration methods: a survey. *Image and Vision Computing*, 21:977–1000, 2003.

[8] B. A. Nickerson, P. A. Fitzhorn, S. K. Koch, and M. Charney. A methodology for near-optimal computational superimposition of two-dimensional digital facial photographs and three-dimensional cranial surface meshes. *Journal of Forensic Sciences*, 36(2):480–500, March 1991.

[9] T. Blickle. Tournament selection. In T. Bäck, D. B. Fogel, and Z. Michalewicz, editors, *Handbook of Evolutionary Computation*, pages C2.3:1–C2.3:4. IOP Publishing Ltd and Oxford University Press, 1997.

[10] K. Deb and R. B. Agrawal. Simulated binary crossover for continuous search space. *Complex Systems*, 9:115–148, 1995.

[11] T. Bäck, D. B. Fogel, and Z. Michalewicz, editors. *Handbook of Evolutionary Computation*. IOP Publishing Ltd and Oxford University Press, 1997.

[12] G. J. Klir and B. Yuan. *Fuzzy sets, fuzzy logic, and fuzzy systems: selected papers by Lotfi A. Zadeh*. World Scientific Publishing Co., Inc., 1996.

[13] P. Diamond and P. Kloeden. Metric topology of fuzzy numbers and fuzzy analysis. In D. Dubois and H. Prade, editors, *Fundamentals of Fuzzy Sets*, The Handbooks of Fuzzy Sets, chapter 11, pages 583–637. Kluwer Academic, 2000.

[14] D. Dubois and H. Prade. On distance between fuzzy points and their use for pausible reasoning. In *International Conference on Systems, Man and Cybernetics*, pages 300–303, 1983.

[15] I. Bloch. On fuzzy distances and their use in image processing under imprecision. *Pattern Recognition*, 32:1873–1895, 1999.

ISBN: 978-989-95079-6-8

Incorporating Fuzziness in Spatial Susceptible-Infected Epidemic Models

Jan M. Baetens Bernard De Baets

KERMIT, Department of Applied Mathematics, Biometrics and Process Control
Ghent University, Coupure Links 653, 9000 Gent, Belgium
Email: jan.baetens@ugent.be, bernard.debaets@ugent.be

Abstract— *In this paper we propose a coupled-map lattice for modelling epidemic spread in a fuzzy setting. The presented model complies with the need for adequate modelling tools to describe and/or predict spatio-temporal phenomena, following the growing availability of spatio-temporal data. Furthermore, our approach does not rely on partial differential equations making it particularly suited to model epidemics in a fuzzy setting. It will be shown that the presented model allows to describe epidemic spread when the magnitude of the initial outbreak and/or the epidemic properties are only imprecisely known.*

Keywords— epidemic, discrete model, fuzzy initial condition, spatio-temporal dynamics

1 Introduction

Ordinary differential equations (ODEs) are widely used and well established to model various biological phenomena, as illustrated extensively in [1]. Partial differential equations (PDEs) are often resorted to if one is not merely interested in the process' temporal dynamics but also in the spatial patterns it generates [2]. Recently, several researchers have addressed the (numerical) solution of fuzzy ODEs (FODEs) [3, 4], endorsed by their potential importance in various scientific fields, for including imprecise information into well-established mathematical models (see [3, 5]). At present, the study of FODEs is still growing [6, 7], while thorough research on fuzzy PDEs is not yet carried out. Two distinct approaches have been developed within the theory of FODEs, differing only in whether they rely upon the notion of fuzzy derivatives or not [8]. This dichotomy and the immaturity of the theory of FODEs and FPDEs might hamper the widespread consideration of fuzziness within mathematical biology, despite often being faced with imprecise information. To overcome these barriers, we propose a coupled-map lattice (CML), developed by [9], to work with fuzzy initial conditions and/or parameters easily in a spatially explicit context. A short overview of fuzziness in discrete dynamical systems will be presented in the first section of this paper. In the second section we will introduce the CML which will be used to model spatio-temporal epidemic dynamics. In the third section we will deal with fuzzy initial conditions, while fuzzy parameters will be treated in the last section.

2 Fuzziness in discrete dynamical systems

A cellular automaton (CA), first introduced by von Neumann and Ulam as 'cellular spaces', and explored in detail by Wolfram [10, 11], is a mathematical model, discrete in all its senses, e.g. space is represented by an infinite lattice of cells, updates occur only at discrete time steps and the states can only take a finite number of values [10]. CA and CML are closely related, but in the latter states can take arbitrary values [12]. Although the first notion of a fuzzy CA dates back to the late 60s [13], literature on fuzzy CA is considered insufficient [14]. Fuzzy automata were first defined by Wee and Fu [13], but several alternative definitions have been proposed [14, 15]. Essentially, every state is attributed a membership value in a fuzzy CA [15], as such relaxing the condition of merely allowing discrete states. Recently, a review on fuzzy automata has been published [14], following the increasing number of articles published on the topic (see [16, 17, 18]). Despite the definition given in [13], fuzzy CA are often simply understood as spatial extensions of fuzzy rule-based models such as Mamdami-Assilian [19, 20] or Takagi-Sugeno models [21], e.g. CA in which the local transition function is a fuzzy rule-based model (see [22, 23, 24, 25, 26, 27]). To our knowledge, the notion of fuzziness in CML models has not been addressed yet.

3 Spatially explicit modelling of epidemics

3.1 The model

Several authors, including Kaneko [12] and Wolfram [11], have argued that CML and CA provide a suitable framework to deal with spatio-temporal dynamics. This is illustrated by the rich variety of such models that has been developed during the last decade for describing various spatial biological phenomena such as epidemics [28, 29, 30], population dynamics [31, 32], tumor growth [33, 34, 35], biofilm development [36, 37] and much other phenomena [38, 39].

Recently, Baetens and De Baets [9] proposed a generalized CML for modelling various biological phenomena, traditionally described by means of PDEs. Their model is general in two senses. Firstly, exploiting graph notations makes it independent from the spatial subdivisions used to discretize the space domain and secondly, it can serve as a basis for modelling various biological phenomena. With regard to an epidemic sweeping through a region which is subdivided into irregular polygons, and involving only non-reproducing susceptible and infected individuals, it can be written in a simplified form as

$$\begin{cases} S_j^{t+1} = S_j^t - S_j^t \displaystyle\sum_{P_k \in N(P_j)} w_{jk}\, G\left(\mathbf{I}_j, d_{jk}\right)\, I_k^t \\ I_j^{t+1} = I_j^t + S_j^t \displaystyle\sum_{P_k \in N(P_j)} w_{jk}\, G\left(\mathbf{I}_j, d_{jk}\right)\, I_k^t \end{cases} \tag{1}$$

where S_j^t, resp. I_j^t, represent the fraction of susceptible, resp. infected individuals within polygon P_j at the t-th time step

ISBN: 978-989-95079-6-8